Atmos. Chem. Phys. Discuss., 10, 22993–23016, 2010
www.atmos-chem-phys-discuss.net/10/22993/2010/
doi:10.5194/acpd-10-22993-2010

Atmospheric Chemistry and Physics Discussions

On the behaviour of the tropopause folding events over the Tibetan Plateau

X. L. Chen[1,2], Y. M. Ma[1], H. Kelder[3], Z. Su[2], and K. Yang[1]

[1]Key Laboratory of Tibetan Environment Changes and Land Surface Processes, Institute of Tibetan Plateau Research, Chinese Academy of Sciences, Beijing, China
[2]Faculty of Geo-Information Science and Earth Observation of the University of Twente, Enschede, The Netherlands
[3]Eindhoven University, Eindhoven, The Netherlands

Received: 27 January 2010 – Accepted: 8 September 2010 – Published: 6 October 2010

Correspondence to: X. L. Chen (chen24746@itc.nl)

Published by Copernicus Publications on behalf of the European Geosciences Union.

Abstract

Due to its harsh natural conditions, there had not been any intensive radiosonde observations over the Tibetan Plateau (TP) until the year 2008, when a regional radiosonde observation network was implemented through a Sino–Japan joint cooperation project. This paper reports new findings on the structure of upper troposphere and lower stratosphere (UTLS) layer, and provides evidence for stratosphere and troposphere exchange (STE) over the TP.

Due to sparseness of high resolution sonde data, many previous studies assumed that there was only one thermal tropopause over the TP. Actually the radiosonde temperature profiles at pre-onset time of the Asian monsoon over the TP often exhibit a multiple tropopause (MT). The MT occurs in winter time with much higher frequency than any previous estimations over the Plateau. The MT during this time period is associated with tropopause folding near the subtropical westerly jet. The MT consistently varied with the movement of the jet. The MT becomes a single tropopause with the development of the monsoon. According to their height distribution, the MT can be divided into tropical and polar characterized tropopauses. Detailed analyses of MT characteristics are reported in this paper. Although some scientists have analyzed global MT events (with data including GPS radio occultation, ERA40 data and Integrated Global Radiosonde Archive database), the frequency of their MT occurrences in winter season over the plateau is largely under-estimated. This significant difference must be caused by the coarse vertical resolution of these data.

The stratospheric intruding episodes are generally associated with the presence of subtropical westerly jet stream over the Plateau. The subtropical jet causes dynamic tropopause foldings over the plateau, which have been observed by us as thermal MT events. Intrusions of high latitude stratospheric ozone rich air into the troposphere over the plateau give us a new explanation to why total column ozone in winter is higher than that in summer.

1 Introduction

The Tibetan Plateau (TP), which has an average height of over 4000 m and an area of 2.5 million square kilometres, exerts profound thermal and dynamic influence on the Asian monsoon and global weather and climate. Little about the structure in the region of the upper troposphere and lower stratosphere (UTLS) over the TP is known. Because of the low air density and strong solar radiation over it, the TP allows more energy from the surface directly heat the middle troposphere. This heat can reaches and warms the tropopause (Fu et al., 2006). The exchange between upper troposphere and lower stratosphere (UTLS) was found significant over the Tibetan Plateau (Cong et al., 2002; Fu et al., 2006; Steinwagner et al., 2007; Zhan and Li, 2008). As a huge elevated heating source (Ye and Gao, 1979), with the dynamical pumping and sucking (Duan et al., 2005), combined with the subtropical westerly jet and rigorous deep convection (Yang et al., 2004), the TP generates an active stratosphere and troposphere exchange (STE) region, forming a short-circuit and pathway for the STE (Fu et al., 2006). A full understanding of the STE depends on our ability to quantify the UTLS structure and its variability (Stohl et al., 2003). We know little about the structures of UTLS over the Tibetan Plateau due to unavailability of high quality observational data, although STE over the Plateau is extremely important.

Meanwhile, satellite observations of ozone have shown "Ozone Mini-Hole" events, and ozone valley phenomena (Zhou and Zhang, 2005; Tobo et al., 2008; Bian 2009). The mechanisms responsible for the low total ozone have been discussed for decades. Previous studies have proven inburst of tropospheric ozone-poor air into stratosphere maintaining lower total ozone in summer (Zhou et al., 1995; Zou, 1996). Tian et al. (2008) found that the low total ozone over the TP is closely related to uplift and descent of isentropic surfaces. Tobo et al. (2008) observed ozone anomalies near the tropopause (150–70 hPa) having a large contribution to the low total ozone. The latest work reminds us that ozone variation at UTLS can contribute to the low total ozone.

ACPD
10, 22993–23016, 2010

Tropopause folding often happens in conditions with upper layer jet (Reed, 1955; Schmidt et al., 2005; Randel et al., 2007). Intrusions of stratospheric rich ozone air into the troposphere were closely associated with tropopause folding (Reed 1955). The Tibetan Plateau is situated at 28–38° N, a latitudinal band where the subtropical westerly jet stream is prevailing. Accompanied with this strong westerly, stratosphere intrusions should frequently happen. These downward transports of rich ozone air strongly influence the vertical ozone distribution especially at UTLS area over the Plateau. However the variation of the stratosphere intrusion and its influence on the vertical ozone distribution are rarely described in detail.

Tian et al. (2008) analyzed the relationship between low total ozone and the cold point tropopause, as well as the thermal tropopause derived from ECMWF ERA40 over the Plateau, presupposing a simple tropopause. Both Añel et al. (2008) (employing Integrate Global Radiosonde Archive database) and Randel et al. (2007) (based on GPS radio occultation measurements and ERA40) derived global statistics of multi-tropopause (MT), but the frequency of their double tropopause (DT) over the Plateau were largely under-estimated when compared to our estimation (see details in following texts). This latter discovery tells us neither of the above data can produce detailed information about thermal structures in the UTLS over the Plateau.

This study will focus on the following relevant issues. (1) What is the detailed UTLS structure over the TP? (2) What are the influences of the westerly jet on intrusions, and the intrusion of stratospheric air on the vertical ozone distribution, further on the total ozone over the plateau?

In order to understand the atmosphere heating and water vapor variations over the TP during different phases of the monsoon, a Sino–Japan joint cooperation project carried out radiosonde intensive observations in 2008 (Xu et al., 2008). As illustrated in Fig. 1, there are nine meteorological radiosonde observation sites involved in the experiment. Four sites (Gerze, Lasha, Nagqu, and Litang) were situated on the Plateau. The other stations were not more than 2000 m a.s.l. (above sea level) and can be taken as observations of low altitude.

ACPD
10, 22993–23016, 2010

As high resolution information about the tropopause over the Plateau has rarely been analyzed before, this study seeks to clarify characteristics of the MT using the most comprehensive radiosonde dataset at present. Section 2 describes observational data and tropopause definition. MT characteristics are presented in Sect. 3. Section 4 explains dynamic tropopause folding which has been observed by radiosonde as thermal MT events. Section 5 summarizes the study with conclusions and discussion.

2 Observation data and tropopause definition

Three sites Gerze, Litang, and Dali were equipped with Vaisala newly developed DigiCORA III GPS radiosonding system. The radiosondes used were Vaisala RS92 calibrated with local meteorological measurements before releasing. The sounding data contained profiles of temperature, pressure, relative humidity, horizontal wind speed and direction. Utilizing differential GPS theory, the receiver can compute vertical height of the sensor and wind information automatically. The radiosonde transmits data downward to the receiver every 2 s. With an average 5 m/s ascending speed, the obtained vertical resolution of the data is about 10 m. The other six sites employed the Chinese meteorological radiosonde system. These systems can observe temperature, pressure, humidity, wind speed and direction every 100 m. All the observation data are interpolated to 20 m vertically equal-spaced levels with cubic splines method for the convenience of detailed analysis and comparison.

Three intensive observation periods (IOP) were carried out. Detailed information about the observation dates are shown in Table 1. The first observation period (IOP1) was aimed at the pre-onset of the monsoon. The second observation period (IOP2) was conducted in the period of monsoon onset time. The third observation period (IOP3) was almost in the mature phase of monsoon. Four radiosondes were released every day at 01:00, 07:00, 13:00 and 19:00 local standard time (LT).

For computing the tropopause height, we employ the WMO lapse rate tropopause (LRT) definition (World Meteorological Organization, 1957):

ACPD

10, 22993–23016, 2010

On the behaviour of the tropopause folding events over the Tibetan Plateau

X. L. Chen et al.

(a) The first tropopause is defined as the lowest level at which the lapse rate decreases to 2 K/km or less, provided also the average lapse rate between this level and all higher levels within 2 km does not exceed 2 K/km.

(b) If above the first tropopause the average lapse rate between any level and all higher levels within 1 km exceeds 3 K/km, then a second tropopause is defined by the same criterion as under (a). This tropopause may be either within or above the 1 km layer.

The first tropopause is denoted by LRT1, and if another tropopause presents upon LRT1, it is named LRT2 and then LRT3. Double tropopause (DT) is denoted by detection of LRT1 and LRT2. Triple tropopause (TT) is identified as profile detected with LRT1, LRT2 and LRT3.

3 Multi-tropopause observed by radiosonde

In previous studies little attention was paid to MT over the plateau, due to lack of radiosonde data. During the intensive observation period, we found a frequent strong inversion layer existing around 10 km above Gerze station (32.09° N, 84.25° E) situated at western Plateau. To testify whether it can be taken as tropopause, we adopted the MT definition of WMO (1957) and proved that MT often happened during IOP1. Examples of the DT temperature profiles from Gerze station are shown in Fig. 2a. Continuous radiosonde data for 25 February 2008, 01:00 LT to 26 February 2008, 13:00 LT are exhibited. The profiles show a tropopause identified around 300 hPa, and a second tropopause detected near 100 hPa. Figure 2b reveals profiles from 29 February 2008, 01:00 to 1 March 2008, 13:00 LT with only one tropopause above 100 hPa. We will explain what causes the difference in UTLS structure in these two time periods in Sect. 4.

Employing the WMO LRT definition to all the stations, we computed MT frequencies of the three IOPs, and listed them in Table 2. The frequency of MT events is given

ACPD
10, 22993–23016, 2010

as a percentage with respect to the number of LRT1 events (Añel et al., 2008). The MT occurrences of the three Plateau stations (Gerze, Nagqu, Litang) for IOP1 are as high as 72 to 84%, which are much higher than those of the GPS occultation data and of the ERA40 data in Randel et al. (2007). The frequency of MT (discussed with Randel) on the plateau was not more than 40% in their Fig. 9a and Fig. A1b. This lower frequency can be attributed to the low vertical resolution of the GPS occultation data and the ERA40 data. Añel et al. (2008) analyzed global MT events performed on the Integrated Global Radiosonde Archive database. As shown in their Fig. 2, the percentage of MT occurrence had less seasonal variation and much lower value than our estimations in winter time. This result can be attributed to shortage of radiosonde data and poor data quality over the TP (their Fig. 1 demonstrated that only the Nagqu site over the plateau was included). At the Dali site, which has an elevation of 1960 m and locates out of the south plateau, the DT occurrence of IOP1 is about 12.9%. This value is much lower than that of other stations. These suggest that when moving to souther low areas, the frequency of MT becomes lower. The MT frequencies of all the plateau stations during IOP3 are the lowest comparing to other two periods. It is therefore concluded that MT occurs in winter time with high frequency over the Plateau.

Figure 3 shows about the statistical distributions of MT height during the three IOP. The statistics for IOP1 demonstrate an overall bimodal distribution with maxima near 10 km (primarily associated with LRT1) and 17 km (firstly contributed by LRT2). LRT1 is more inclined to polar tropopause characteristics than to tropical tropopause characteristics during this time. The majority of LRT2 height in IOP1 is around 17 km, which is more close to equatorial tropopause. The statistics of IOP2 and IOP3 in Fig. 3 show a single maximum (primarily LRT1) centred near 17 km, which means MT is rarely observed during the monsoon season.

Khalili (1975) pointed out that ten days average tropopause height has high negative correlation coefficient with its temperature. We also analyzed the relationships between the tropopause height and temperature. LRT1 and LRT2 heights are in opposite phase with their temperature in hours scale as shown in Fig. 4. LRT3 doesn't show this

ACPD
10, 22993–23016, 2010

character suggesting itself as an stratospheric inversion layer. On the contrary, LRT1 and LRT2 should be attributed to tropospheric inversion layer.

The average heights of DT during the three periods are listed in Table 3. LRT1 of the three plateau stations (Gerze, Nagqu and Litang) have heights around 11–13 km during IOP1. These tropopauses can be treated as polar characteristic tropopauses (which usually have heights around 9 km). Regardless of the observation periods and sites they are, LRT2 is more similar to tropical tropopause (around 17 km). After the monsoon onset, the LRT1 height over the Plateau was elevated with 4–5 km to be merged with the LRT2, indicating the disappearance of the polar characteristic tropopause. This can be easily explained as a result of plateau's thermal forcing, which cause large-scale ascent flow and vertical convection. Tian et al. (2008) suggested the thermal sink (source) prevailing the descent (ascent) flow lower (lift) the tropopause. The thermal dynamic effects of the plateau can be one reason of seasonal variation of the tropopause, but can not explain the LRT1 height variation between 10–17 km before monsoon. Our explanation is presented in the next part.

4 The tropopause fold over the Tibetan Plateau

It is well known that altitude variation of tropopause in the extratropics has close relationship with local synoptic situation. In order to understand simultaneous meteorological situation, we use the ECMWF ERA40 reanalysis data to analyze atmosphere structure associated with the simple tropopause and DT profiles in Fig. 2. We take 25 February 2008, 12:00 LT (Fig. 5a) and 29 February 2008, 12:00 LT (Fig. 5b) as examples. During these two times, DT and simple tropopause were observed both at Gerze and Nagqu. Figure 5 includes potential vorticity (PV) isolines (units: $10^{-6}\,\mathrm{K\,m^2\,kg^{-1}\,s^{-1}}$), zonal wind and potential temperature derived from ERA40 data. Inverted triangles show simultaneous tropopause height observed by the two stations. In order to exactly locate their position in the figure, we interpolated the ERA40 1.5° latitudinal resolution to 0.1°, and pressure levels lower than 400 hPa to 10 hPa, higher than 400 hPa to 25 hPa vertical resolution.

ACPD

10, 22993–23016, 2010

An alternative definition of tropopause is to use PV. We draw a series of PV isolines (PV=1–5 unit) to indicate the approximate location of the dynamical tropopause (blue lines in Fig. 5). A principal indicator of ingress of stratospheric air into troposphere is the occurrence of an anomalous high PV value reaching down towards middle tropospheric height. It is because PV is generally greater in the stratosphere than in the troposphere (Holton 2004). Contour lines of zonal wind in Fig. 5a show that westerly jet stream runs along the 30° N latitude right above the TP. The maximum wind speed is higher than 70 m/s at 200 hPa level. The PV isolines were distorted to closely abutted upon the northern edge of the subtropical jet stream. The 2 PV isoline has been deeply curved down to 380 hPa over the Plateau. A strong folding around 30° N is identified with isentropic layers between 300 K and 340 K plunging into the troposphere in Fig. 5a. The PV tropopause (identified by the PV=1–5 isolines) does exhibit a strongly folded structure over the Plateau. It indicates a strong stratospheric intrusion happening over there. The entrainment of stratospheric air within the folds is marked not only by high values of PV but also by rich ozone air mass. The trace gas or content were transported by downward meridional wind at the north edge of the jet core as shown in Fig. 6. Another tropopause fold occurred around 60° N at the same time.

We plot a similar meteorologic situation at 29 February 2008, 12:00 LT (Fig. 5b) to interpret simple tropopause observed at that time in detail. The jet core moved northward to 34° N, at north of Gerze and Nagqu site. The slightly folded structure at this time was pulled to north of the Plateau. The equatorial tropopause extends over the south plateau. The dynamic tropopause becomes smoothly without folds over the two stations. Thus the radiosondes at this time observed only one thermal tropopause at both the stations. According to the analysis at these two times, the tropopause folding follows the displacement of the subtropical westerly jet running over the Plateau.

We have analyzed the jet core position in both periods in Fig. 2 (not shown). The jet core situated around 28° N at south of Gerze, from 25 February 2008, 0:00 to 26 February 2008, 13:00 LT. The strong tropopause folding following it leads to DT events observed by the radiosonde at Gerze (Fig. 2a). During the simple tropopause periods

ACPD
10, 22993–23016, 2010

from 29 February 2008, 01:00 to 1 March 2008, 13:00 LT in Fig. 2b, the jet moves to near 33° N, northern than Gerze. The tropopause folding moves further northward correspondingly and becomes weaker than that of double tropopause period. Equatorial tropopause intrudes over the station, which was represented by simple thermal tropopause in this period.

Stratospheric intrusion is highly likely to occur under tropopause folding structure. Scientists have discovered that frequent descent air circulation over the Plateau during winter season (e.g., Yanai et al., 1992). This flow more strongly favours stratospheric intrusions into troposphere more easily in winter. The intrusion of rich ozone air from higher latitude stratosphere to the plateau troposphere in winter are more frequent than in summer. This effects cause total ozone value in winter higher than that of summer. Scientists have described this phenomena as middle tropospheric ozone minimum in June (Liu et al., 2009), and relatively low ozone mixing ratios extending from the troposphere to the lower stratosphere (Tobo et al., 2008). These two phenomena can also be explained as less downward transport of stratospheric rich ozone air in summer than in winter.

To further investigate the observed close relationship between the jets and tropopause folds above, we display the seasonal variations of the jets (Fig. 7) to explain seasonal difference in tropopause structure. Subtropical jet is strengthened by the cooling effect of the Plateau (Ye and Gao, 1979), and locates at the south of the Plateau during winter season. The Dali station (25° N) has notably lower frequency of MT all year around (in Table 2), which can be attributed to the scarce southward movement of the westerly jet passing the latitude of the station. With the development of the plateau monsoon, subtropical westerly jet weakens and retreats to the north of the Plateau. During the month of July the jet stream axis moves north to around 40° N. The influence of the north movement of the jet has been noted by Ding et al. (2006). Their study attributed summertime maximum O_3 events at Waliguan (36.28° N, 100.90° E, in north of the Plateau) to stratospheric intrusions, which were generally associated with upper-level jet streams over there.

ACPD
10, 22993–23016, 2010

The south-northward movements of the jet streams cause the latitudinal variation of tropopause folds, which finally determine the simple or multi tropopauses observed at the plateau stations. Thus we have observed two distinctive peak values in LRT1 height distribution. The westerly jet induced tropopause folds is the main reason for height variation of LRT1 in winter. Its northward retreat in summer is the cause of the observed single tropopause during IOP2 and IOP3. The stable tropical characteristic tropopause existing above the south plateau in summer should be attributed to poleward extending of tropical tropopause over there (Pan et al., 2009).

5 Discussion and conclusions

LRT1 over the Plateau has polar and tropical tropopause characters during the winter, and has a consistent tropical tropopause character in summer. This complexity causes difficulty in determining the exact heights of tropopause over the TP. When only one tropopause is premised, only the LRT1 characteristic as observed in our paper can be captured. For example, Tian et al (2008) reported the retrieved tropopause in the ERA40 data in summer was higher than that in winter which was actually similar to variation of the LRT1. Schmidt et al. (2005) also discovered a bimodal distribution of the lowest LRT (equal to LRT1) altitude between 30° N–50° N employing GPS radio occultation data. While these data have furthered our knowledge about global and climatic characteristics of UTLS, the lower statistics of MT using present GPS and ERA40 data have testified their inability to capture more tropopause inversion layers.

The PV tropopause exhibits a strongly folded structure around the subtropical jet. This folded structure has been observed by radiosonde observation over the Plateau. We found frequent intrusions of stratospheric air in the spring time over the Plateau which has received little attention so far. Our results also enable a different explanation to the low total ozone in summer. The reduced down-transporting of stratospheric rich ozone air also contributes partially to the low total ozone.

ACPD
10, 22993–23016, 2010

Title Page
Abstract | Introduction
Conclusions | References
Tables | Figures
◄ | ►
◄ | ►
Back | Close
Full Screen / Esc
Printer-friendly Version
Interactive Discussion

The lack of high resolution information of the vertical atmosphere has hampered our knowledge about tropopause characteristics so far. More radiosonde data with high vertical resolution are indispensible to further quantify tropopause structure and variability. Discovering previous lower estimation of MT frequency, this work could further deepen our understanding in UTLS structure over the Plateau. Our study has also demonstrated that the radiosonde data are still the principal source of information regarding the thermal structure of UTLS.

Supplementary material related to this article is available online at: http://www.atmos-chem-phys-discuss.net/10/22993/2010/ acpd-10-22993-2010-supplement.zip.

Acknowledgement. We appreciate constructive comments from reviewers. This research was funded by the Chinese National Natural Science Foundation (40825015 and 40810059006), EU-FP7 project "CEOP-AEGIS" (212921), and the Sino-Japan JICA project. Xuelong Chen is supported by the "CAS-KNAW Joint PhD Training Programme". The authors thank all the participants from China and Japan for their very hard field work during the JICA Tibetan Plateau meteorological observations. We thank Laura L. Pan, Cameron Homeyer, J. A. Añel, and William J. Randel for their kind help and discussions during the course of this work. ERA40 data were provided by the European Centre for Medium-Range Weather Forecasts (ECMWF).

References

Añel, J. A., Antuña, J. C., de la Torre, L., Castanheira, J. M., and Gimeno, L.: Climatological features of global multiple tropopause events, J. Geophys. Res., 113, D00B08, doi:10.1029/2007JD009697, 2008.

Bian, J.: Features of ozone mini-hole events over the Tibetan Plateau, Adv. Atmos. Sci., 26(2), 305–311, 2009.

Cong, C. H., Li, W. L., and Zhou, X. J.: Mass exchange between stratosphere and troposphere over the Tibetan Plateau and its surroundings, Chinese Sci. Bull., 47, 508–512, 2002.

Ding, A. and Wang, T.: Influence of stratosphere-to-troposphere exchange on the seasonal cycle of surface ozone at Mount Waliguan in Western China, Geophys. Res. Lett., 33, L03803, doi:10.1029/2005GL024760, 2006.

Duan, A. M. and Wu, G. X.: Role of the Tibetan Plateau thermal forcing in the summer climate patterns over subtropical Asia, Clim. Dynam., 24(7), 793–807, 2005.

Fu, R., Hu, Y., Wright, J. S., Jiang, J. H., Dickinson, R. E., Chen, M., Filipiak, M., Read, W. G., Waters, J. W., and Wu, D. L.: Short circuit of water vapor and polluted air to the global stratosphere by convective transport over the Tibetan Plateau, P. Natl. Acad. Sci. USA, 103(15), 5664–5669, 2006.

Holton, J. R.: An Introduction to Dynamic Meteorology, 4th Edition, Elsevier Academic Press, 2004.

Khalili, A.: Some characteristics of the tropopause over Tehran, Pure Appl. Geophys., 113(1), 365–374, 1975.

Liu, Y., Wang, Y., Liu, X., Cai, Z., and Chance, K.: Tibetan middle tropospheric ozone minimum in June discovered from GOME observations, Geophys. Res. Lett., 36, L05814, doi:10.1029/2008GL037056, 2009.

Pan, L. L., Randel, W. J., Gille, J. C., Hall, W. D., Nardi, B., Massie, S., Yudin, V., Khosravi, R., Konopka, P., and Tarasick, D.: Tropospheric intrusions associated with the secondary tropopause, J. Geophys. Res., 114, D10302, doi:10.1029/2008JD011374, 2009.

Randel, W. J., Seidel, Dian, J., and Pan, L. L.: Observational characteristics of double tropopauses, J. Geophys. Res., 112, D07309, doi:10.1029/2006jd007904, 2007.

Reed, R. J.: A study of a characteristic type of upper-level frontogenesis, J. Atmos. Sci., 12(3), 226–237, 1955.

Schmidt, T., Heise, S., Wickert, J., Beyerle, G., and Reigber, C.: GPS radio occultation with CHAMP and SAC-C: global monitoring of thermal tropopause parameters, Atmos. Chem. Phys., 5, 1473–1488, doi:10.5194/acp-5-1473-2005, 2005.

Steinwagner, J., Milz, M., von Clarmann, T., Glatthor, N., Grabowski, U., Höpfner, M., Stiller, G. P., and Röckmann, T.: HDO measurements with MIPAS, Atmos. Chem. Phys., 7, 2601–2615, doi:10.5194/acp-7-2601-2007, 2007.

Stohl, A., Bonasoni, P., Cristofanelli, P., Collins, W., Feichter, J., Frank, A., Forster, C., Gerasopoulos, E., Gaggeler, H., and James, P.: Stratosphere-troposphere exchange: a review and what we have learned from STACCATO, J. Geophys. Res., 108(D12), 8516, doi:10.1029/2002JD002490, 2003.

ACPD

10, 22993–23016, 2010

On the behaviour of the tropopause folding events over the Tibetan Plateau

X. L. Chen et al.

Tian, W., Chipperfield, M., and Huang, Q.: Effects of the Tibetan Plateau on total column ozone distribution, Tellus B, 60(4), 622–635, 2008.

Tobo, Y., Iwasaka, Y., Zhang, D., Shi, G., Kim, Y.-S., Tamura, K., and Ohashi, T.: Summertime "ozone valley" over the Tibetan Plateau derived from ozonesondes and EP/TOMS data, Geophys. Res. Lett., 35, L16801, doi:10.1029/2008GL034341, 2008.

Xu, X., Zhang, R. H., Koike, T., Lu, C. G., Shi, X. H., Zhang, S. J., Bian, L. G., Cheng, X. H., Li, P. Y., and Ding, G. A.: A new integrated observational system over the Tibetan Plateau, Bull. Am. Meteorol. Soc., 89(10), 1492–1496, 2008.

Yanai, M., Li, C., and Song, Z.: Seasonal heating of the Tibetan Plateau and its effects on the evolution of the Asian summer monsoon, J. Meteorol. Soc. Jpn., 70, 319–351, 1992.

Yang, K., Koike, T., Fujii, H., Tamura, T., Xu, X., Bian, L., and Zhou, M.: The daytime evolution of the atmospheric boundary layer and convection over the Tibetan Plateau: observations and simulations, J. Meteorol. Soc. Jpn., 82, 1777–1792, 2004.

Ye, D. and Gao, Y.: The Meteorology of the Qinghai-Xizang (Tibet) Plateau (in Chinese), Science Press, Beijing, 62–257, 1979.

Zhan, R. F. and Li, J. P.: Influence of atmospheric heat sources over the Tibetan Plateau and the tropical western North Pacific on the inter-decadal variations of the stratosphere-troposphere exchange of water vapor, Sci. China Ser. D, 51(8), 1179–1193, 2008.

Zhou, S. and Zhang, R.: Decadal variations of temperature and geopotential height over the Tibetan Plateau and their relations with Tibet ozone depletion, Geophys. Res. Lett., 32, L18705, doi:10.1029/2005GL023496, 2005.

Zhou, X., Lou, C., Li, W. L., and Shi, J. E.: Ozone changes over China and low center over Tibetan Plateau, Chin. Sci. Bull., 40, 1396–1398, 1995.

Zou, H.: Seasonal variation and trends of TOMS ozone over Tibet, Geophys. Res. Lett., 23, 1029–1032, 1996.

World Meteorological Organization: Meteorology: A three dimensionalscience, WMO Bull., 6, 134–138, 1957.

ACPD
10, 22993–23016, 2010

On the behaviour of the tropopause folding events over the Tibetan Plateau

X. L. Chen et al.

Table 1. Intensive observation dates of the three periods. X means no observation data.

	Gerze	Lasha	Nagqu	Litang	Lijiang	Dali	Tengchong	Kunming	Mengzi
IOP1	25 Feb–19 Mar	X	25 Feb–19 Mar	07 Mar–16 Mar	X	07 Mar–15 Mar	X	X	X
IOP2	13 May–12 Jun	X	X	13 May–22 May	X	13 May–22 May	X	X	X
IOP3	07 Jul–16 Jul	20 Jun–19 Jul	X	06 Jul–16 Jul	20 Jun–19 Jul	06 Jul–16 Jul	20 Jun–19 Jul	20 Jun–19 Jul	20 Jun–19 Jul

Table 2. Frequency of double tropopause (DT) and triple tropopause (TT) during the three observation periods. X means no observation data.

	Gerze		Lasha		Nagqu		Litang		Lijiang		Dali		Tengchong		Kunming		Mengzi	
	DT	TT	DT	TT	DT	TT	DT	TT	DT	TT	DT	TT	DT	TT	DT	TT	DT	TT
IOP1	44%	40%	X	X	51%	27.6%	51.5%	21%	X	X	12.9%	0%	X	X	X	X	X	X
IOP2	11%	1%	X	X	X	X	2.5%	0%	X	X	13.1%	0%	X	X	X	X	X	X
IOP3	0%	0%	2.5%	0%	X	X	2.6%	0%	4.2%	0%	2.5%	0%	4.2%	0%	5%	0%	4.7%	0%

Table 3. Average height of LRT during the three observation periods. X means no observation data.

	Gerze		Lasha		Nagqu		Litang		Lijiang		Dali		Tengchong		Kunming		Mengzi	
	LRT1	LRT2	LRT1	LRT2	LRT1	LRT2	LRT1	LRT2	LRT1	LRT2	LRT1	LRT2	LRT1	LRT2	LRT1	LRT2	LRT1	LRT2
IOP1	12 359 m	16 914 m	X	X	11 976 m	16 789 m	13 041 m	16 890 m	X	X	16 193 m	18 185 m	X	X	X	X	X	X
IOP2	16 470 m	17 335 m	X	X	X	X	17 338 m	17 980 m	X	X	16 962 m	17 468 m	X	X	X	X	X	X
IOP3	17 289 m	X	16 734 m	17 568 m	X	X	16 885 m	17 860 m	16 948 m	17 662 m	16 862 m	17 960 m	16 925 m	17 636 m	16 887 m	17 283 m	16 459 m	16 106 m

ACPD
10, 22993–23016, 2010

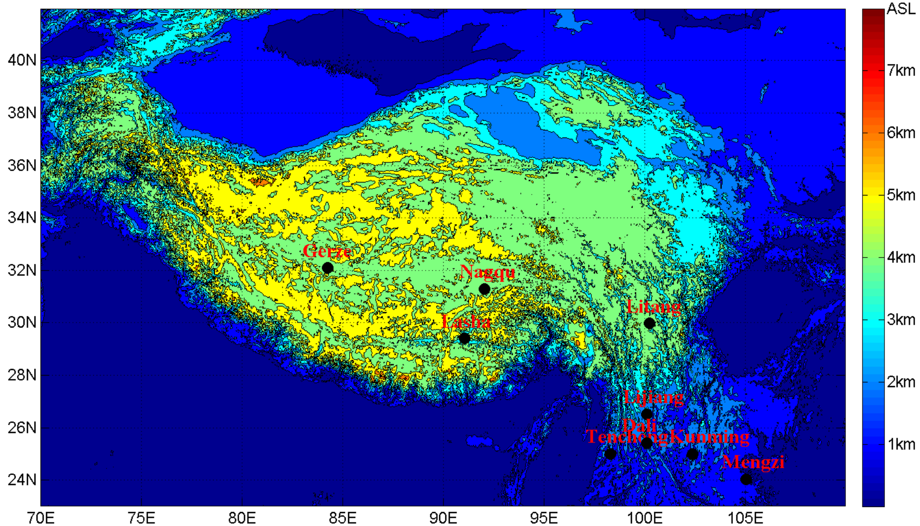

Fig. 1. Distribution of radiosonde sites over the Tibetan plateau (ASL elevation above sea level).

ACPD
10, 22993–23016, 2010

On the behaviour of the tropopause folding events over the Tibetan Plateau

X. L. Chen et al.

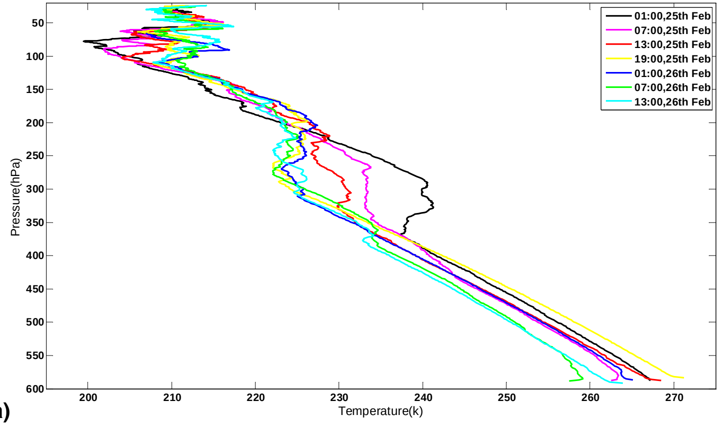

(a)

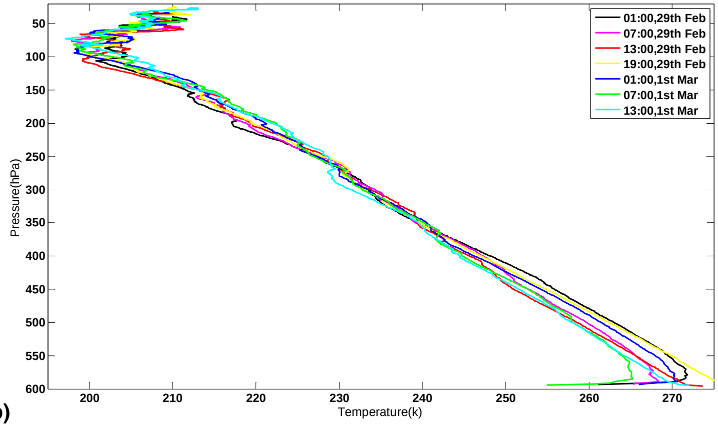

(b)

Fig. 2. (a) Temperature profiles from 25 February 2008, 01:00 to 26 February 2008, 13:00 LT at Gerze site. **(b)** Temperature profiles from 29 February 2008, 01:00 to 1 March 2008, 13:00 LT at Gerze site.

ACPD
10, 22993–23016, 2010

On the behaviour of the tropopause folding events over the Tibetan Plateau

X. L. Chen et al.

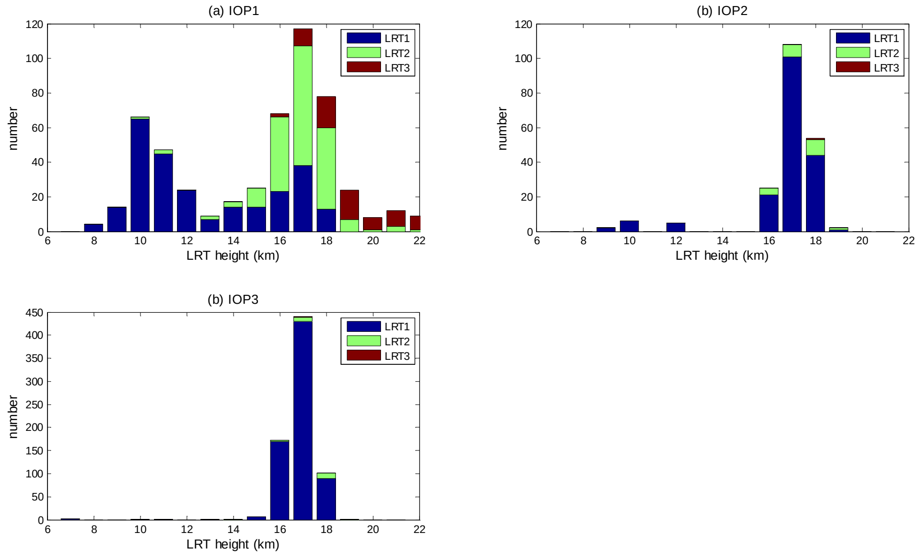

Fig. 3. Distribution of multi-tropopause heights at different phase of the monsoon. The first tropopause (LRT1), second tropopause (LRT2) and third tropopause (LRT3) are displayed by blue, green and brown color separately. Table 1 lists which sites and data are analyzed in these three IOP.

ACPD
10, 22993–23016, 2010

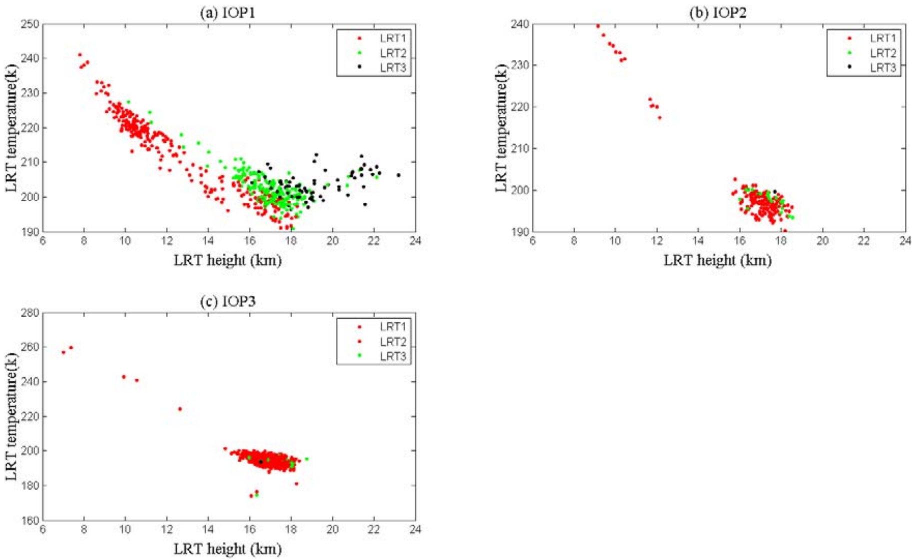

Fig. 4. Multi-tropopause heights versus temperature. The first tropopause (LRT1), second tropopause (LRT2) and third tropopause (LRT3) are displayed by red, green and dark color separately. Table 1 lists which sites and data are analyzed in these three IOP.

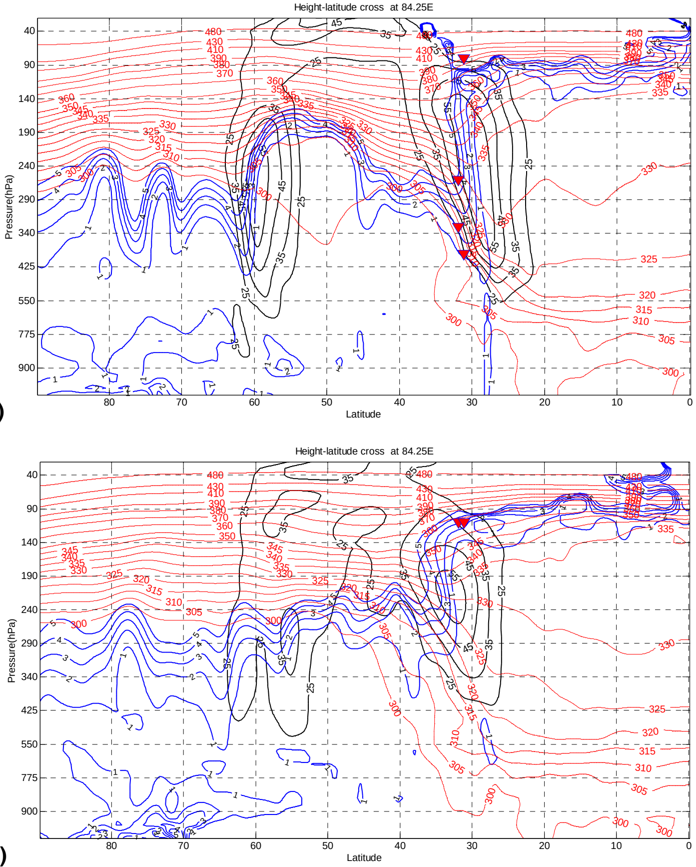

(a)

(b)

Fig. 5. **(a)** Meridional cross-section at 84.25° E (over Gerze site) on 25 February 2008, 12:00 LT between 0 and 90° N in latitude and between 1000 hPa and 20 hPa in the vertical derived from ERA40 data, including zonal winds (black contours, m/s), potential vorticity (PV) (blue lines, contours of 1–5 PV units), and potential temperature (red contours, k). **(b)** same as **(a)** but for 29 February 2008, 12:00 LT.

ACPD
10, 22993–23016, 2010

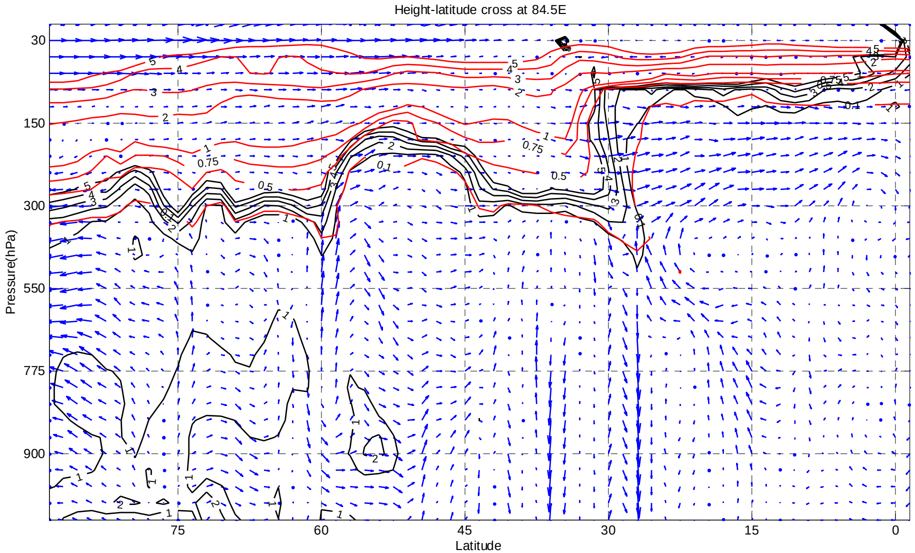

Fig. 6. Height–latitude cross section of meridional wind vector (blue arrow, m/s), ozone mass mixing ratio (red contours, 10^{-6} kg/kg) and potential vorticity (PV) (black lines, contours of 1–5 PV units) at 84.25° E (over Gerze site) on 25 February 2008, 12:00 LT between 0 and 90° N in latitude and between 1000 hPa and 20 hPa in the vertical derived from ERA40 data. The wind vector shows meridional divergent wind (m/s) with vertical velocity (Pa/s) exaggerated by 60 times.

ACPD
10, 22993–23016, 2010

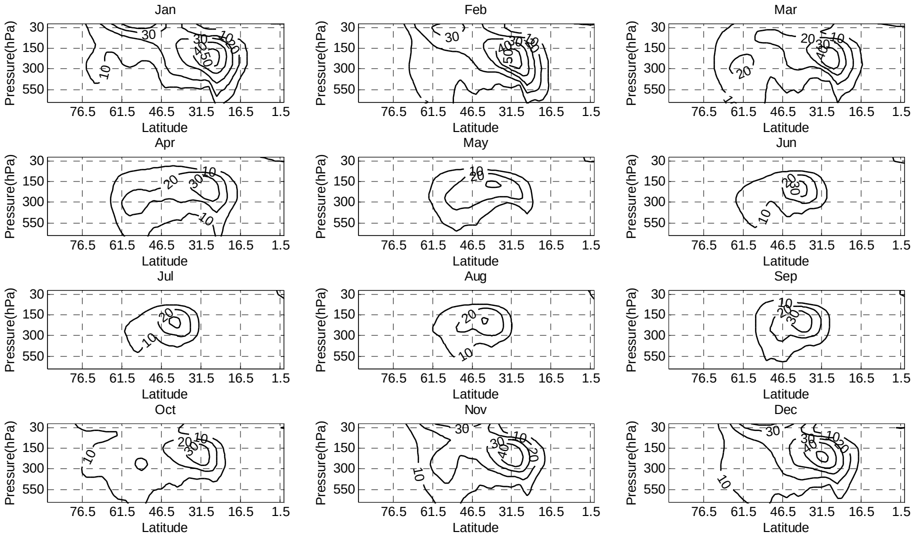

Fig. 7. Height–latitude cross section of zonal wind (m/s) at 90° E between 0 and 90° N in latitude and between 1000 hPa and 20 hPa in the vertical derived from ERA40 data of 2008.

ACPD
10, 22993–23016, 2010

On the behaviour of the tropopause folding events over the Tibetan Plateau

X. L. Chen et al.